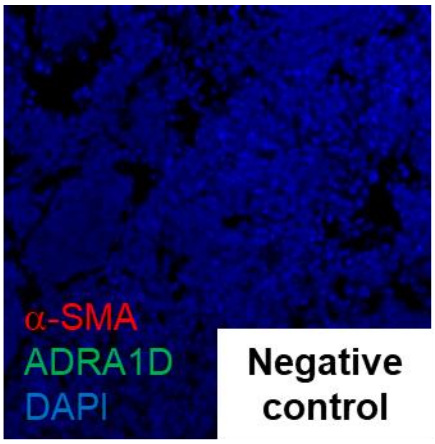

Figure S1 Negative control for immunofluorescence imaging, which involved the omission of primary antibodies, showed the staining of α-SMA (red), ADRA1D (green), and DAPI (blue) in wild-type mouse lung. The images were captured at an original magnification of 20x. ADRA1D, α1-adrenoreceptor subtype D; α-SMA, alpha-smooth muscle actin; DAPI, 4′,6-diamidino-2-phenylindole.

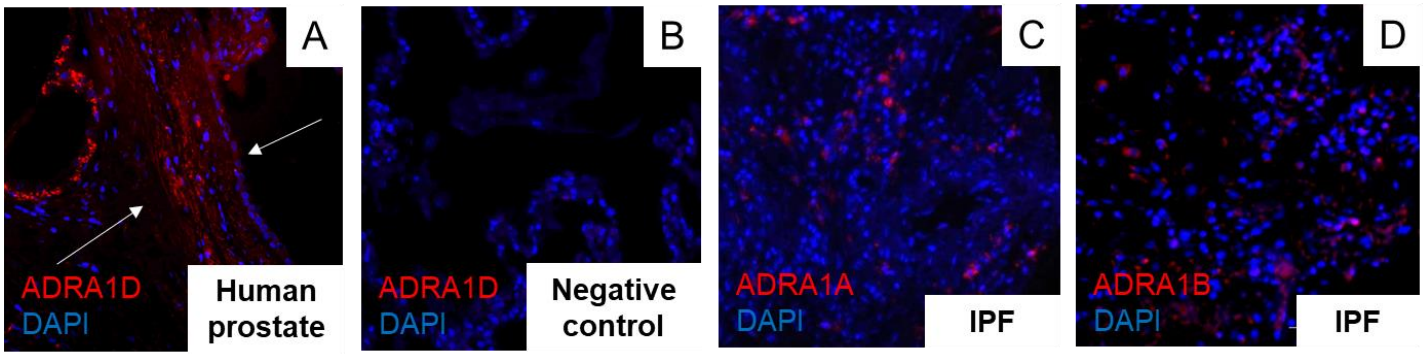

Figure S2: Immunofluorescence analysis of α1-adrenoreceptor expression in human tissues. Immunofluorescence imaging demonstrates α1-adrenoreceptor (red) and DAPI (blue) staining in lung explant tissues from IPF patients, alongside normal lung and normal human prostate tissues. (A) Human prostate tissue serves as a positive control, showing pronounced ADRA1D signal in morphologically characteristic smooth muscle cells (white arrows). (B) Negative control without primary antibodies in normal human lung tissue, confirming absence of ADRA1D expression. (C) Minimal expression of ADRA1A in fibrotic lung tissues. (D) Low expression of ADRA1B in the same tissues. Images were captured at 20x original magnification. ADRA1A, α1-adrenoreceptor subtype A; ADRA1B, α1-adrenoreceptor subtype B; ADRA1D, α1-adrenoreceptor subtype D; DAPI, 4′,6-diamidino-2-phenylindole; IPF, idiopathic pulmonary fibrosis.

Figure S3 (A) Mice engineered with an α-SMA cell-specific knockout strategy (*Acta2-CreERT2; Adra1d*$^{f/f}$), which received tamoxifen or vehicle timed to delete ADRA1D before bleomycin administration. (B) Specific deletion of ADRA1D in α-SMA-expressing cells did not result in reduced collagen deposition. Data are presented as median ± IQR, with statistical test using Mann-Whitney test. ADRA1D, α1-adrenoreceptor subtype D; α-SMA, alpha-smooth muscle actin.

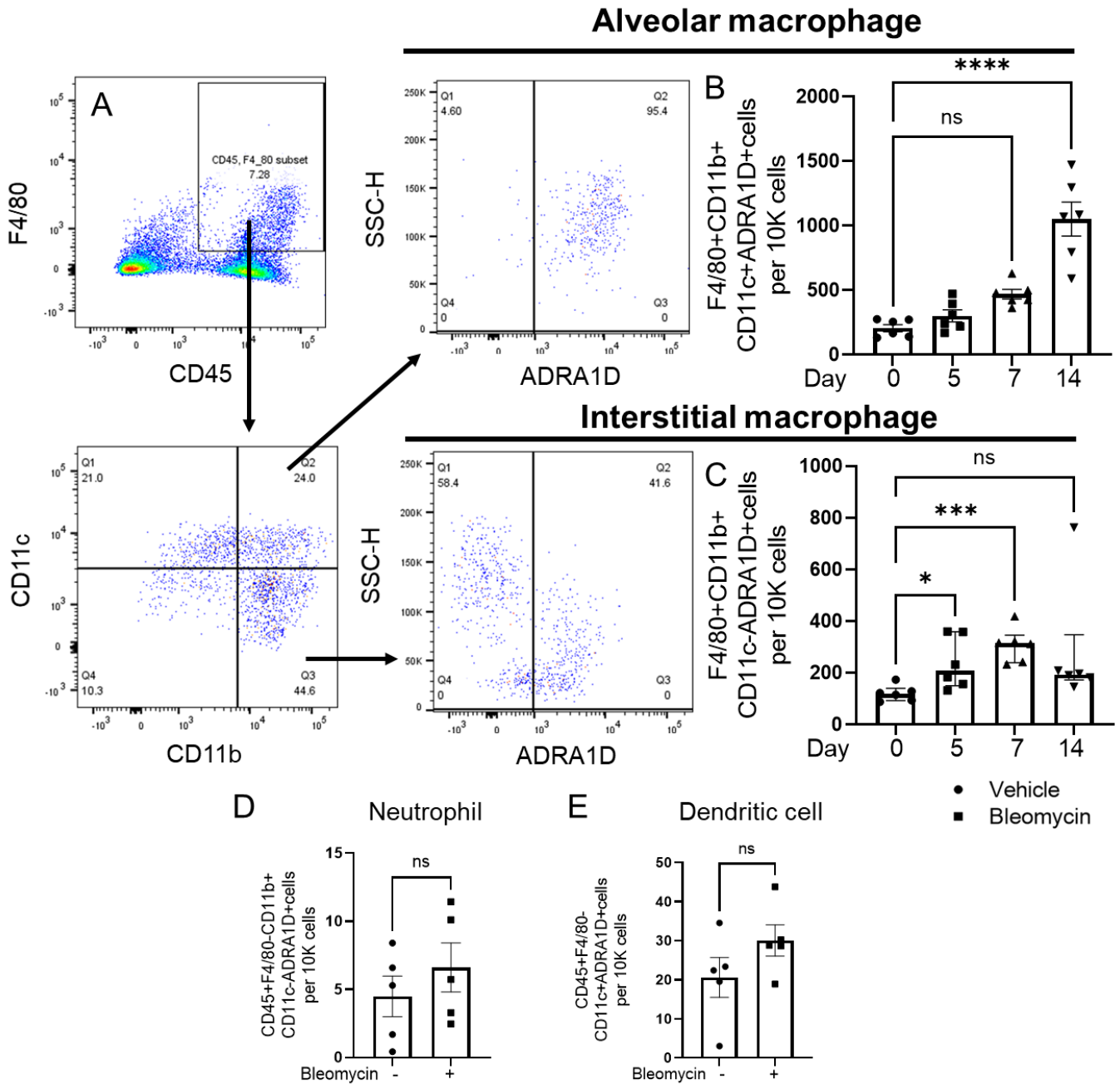

Figure S4: Accumulation of ADRA1D-expressing lung macrophages in bleomycin-challenged mice. (A-C) Wild-type mice received an orotracheal dose of 2.0 U/kg bleomycin and were euthanized on Days 0, 5, 7, and 14 for flow cytometry analysis (A). ADRA1D-expressing alveolar macrophages began accumulating by Day 7 and peaked by Day 14 (B, $P < 0.0001$) while ADRA1D-expressing interstitial macrophages peaked on Day 7 (C, $P = 0.0008$). (D, E) No significant differences were noted in the accumulation of non-macrophage myeloid cells, such as neutrophils (D) and dendritic cells (E), expressing ADRA1D between the bleomycin-treated and control groups. Data are presented as mean ± SEM or median ± IQR, as applicable, with statistical analyses performed using Student's t-test or ANOVA with Tukey's multiple comparisons for normally distributed data, and Kruskal-Wallis tests with Dunn's multiple comparisons for non-normally distributed data. *$P < 0.05$, ***$P < 0.001$, ****$P < 0.0001$.

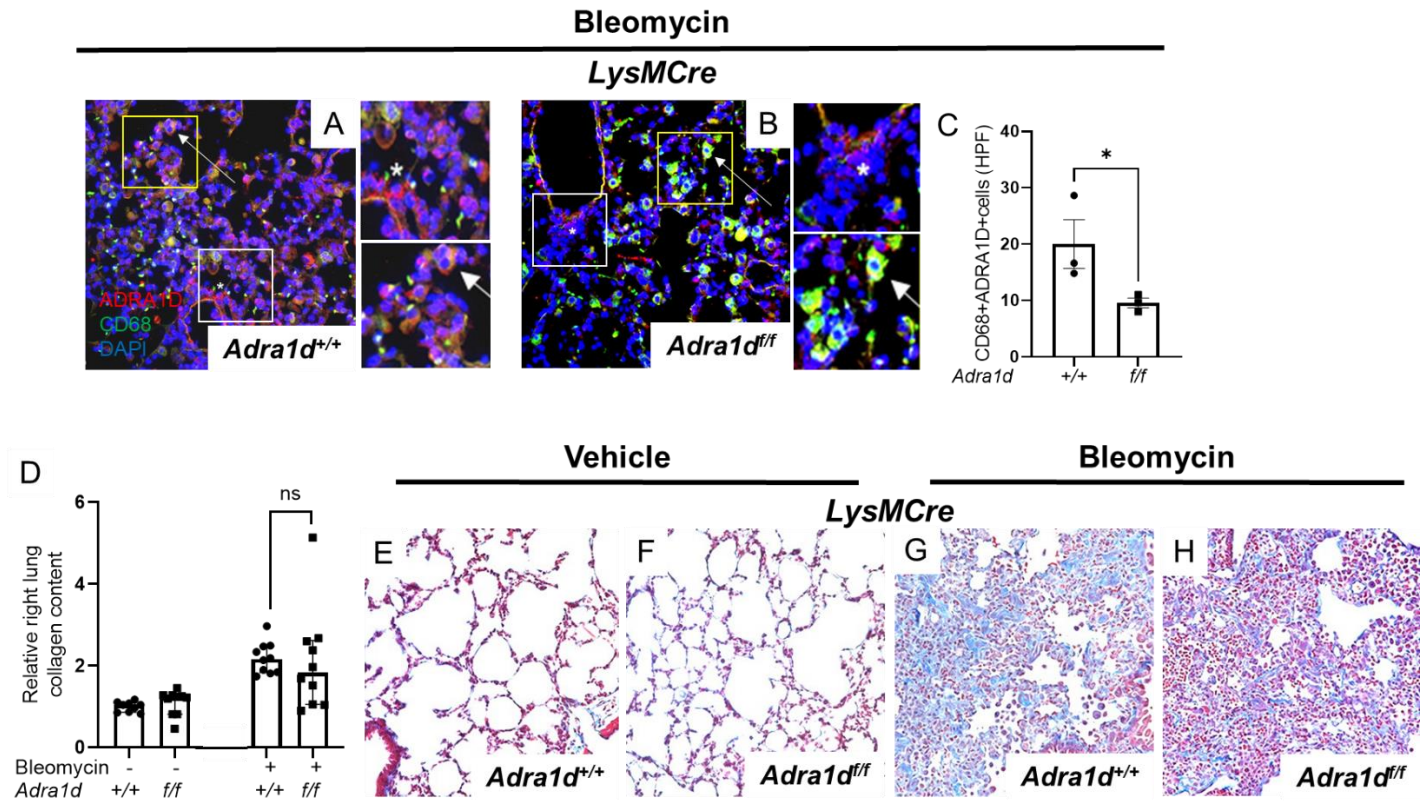

Figure S5: α1-adrenergic signaling in myeloid cells is dispensable for bleomycin-induced lung fibrosis. Utilizing a myeloid-specific knockout approach, *LysMCre* mice were crossed with *Adra1d*$^{f/f}$ mice to produce *LysMCre; Adra1d*$^{f/f}$ offspring. (A-C) Immunofluorescence imaging at 20x magnification displays ADRA1D (red), CD68 (green), and DAPI (blue) in lung tissues on Day 14 post-bleomycin exposure. ADRA1D-intact *LysMCre* mice showed notable macrophage accumulation expressing ADRA1D (white arrows) and ADRA1D expression in structural cells near airways (white asterisks) (A). In contrast, *LysMCre; Adra1d*$^{f/f}$ mice exhibited a significant reduction in ADRA1D-expressing CD68+ macrophages (B, C, $P = 0.0384$), though ADRA1D expression in nearby structural cells was maintained (white asterisks). (D-H) Myeloid-specific deletion of *Adra1d* did not prevent collagen accumulation following bleomycin treatment (D) nor improve outcomes in trichrome staining (E-H). Data are presented as mean ± SEM or median ± IQR, with statistical analyses conducted using Student's t-test for normally distributed data and the Mann-Whitney test for non-normally distributed data. *$P < 0.05$. ADRA1D, α1-adrenoreceptor subtype D; DAPI, 4′,6-diamidino-2-phenylindole.

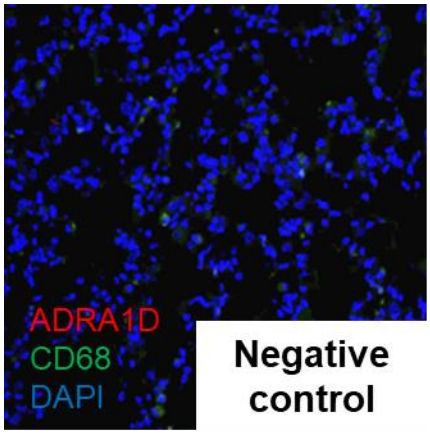

Figure S6 Negative Control for Immunofluorescence Imaging. This control involved the omission of primary antibodies to validate the specificity of the staining for ADRA1D (red), CD68 (green), and DAPI (blue) in mouse lung tissue. Images were captured at an original magnification of 20x, confirming the absence of nonspecific staining. ADRA1D, α1-adrenoreceptor subtype D; DAPI, 4′,6-diamidino-2-phenylindole.